Thermal conductivity of pure silica MEL and MFI zeolite thin films

Thomas Coquil,[1] Christopher M. Lew,[2] Yushan Yan,[2,a)] and Laurent Pilon[1,b)]
[1]*Department of Mechanical and Aerospace Engineering, Henry Samueli School of Engineering and Applied Science, University of California–Los Angeles, 420 Westwood Plaza, Los Angeles, California 90095, USA*
[2]*Department of Chemical and Environmental Engineering, Bourns College of Engineering, University of California–Riverside, Riverside, California 92521-0403, USA*

(Received 4 March 2010; accepted 12 June 2010; published online 16 August 2010)

This paper reports the room temperature cross-plane thermal conductivity of pure silica zeolite (PSZ) MEL and MFI thin films. PSZ MEL thin films were prepared by spin coating a suspension of MEL nanoparticles in 1-butanol solution onto silicon substrates followed by calcination and vapor-phase silylation with trimethylchlorosilane. The mass fraction of nanoparticles within the suspension varied from 16% to 55%. This was achieved by varying the crystallization time of the suspension. The thin films consisted of crystalline MEL nanoparticles embedded in a nonuniform and highly porous silica matrix. They featured porosity, relative crystallinity, and MEL nanoparticles size ranging from 40% to 59%, 23% to 47% and 55 nm to 80 nm, respectively. PSZ MFI thin films were made by *in situ* crystallization, were *b*-oriented, fully crystalline, and had a 33% porosity. Thermal conductivity of these PSZ thin films was measured at room temperature using the 3ω method. The cross-plane thermal conductivity of the MEL thin films remained nearly unchanged around 1.02 ± 0.10 W m^{-1} K^{-1} despite increases in (i) relative crystallinity, (ii) MEL nanoparticle size, and (iii) yield caused by longer nanoparticle crystallization time. Indeed, the effects of these parameters on the thermal conductivity were compensated by the simultaneous increase in porosity. PSZ MFI thin films were found to have similar thermal conductivity as MEL thin films even though they had smaller porosity. Finally, the average thermal conductivity of the PSZ films was three to five times larger than that reported for amorphous sol-gel mesoporous silica thin films with similar porosity and dielectric constant. © *2010 American Institute of Physics*. [doi:10.1063/1.3462500]

I. INTRODUCTION

Low-dielectric constant (low-*k*) materials are essential to the improvement of device density and performance of very large scale integrated (VLSI) circuits.[1–4] The objective is to synthesize dielectric materials with dielectric constants lower than 2.0 to reduce (i) the RC time delay constant, (ii) cross-talk noise, and (iii) power consumption.[5] Pure silica zeolites (PSZs) are crystalline microporous silica materials featuring organized networks of subnanometer micropores. They were found to have a dielectric constant as low as 1.5 thanks to the large microporosity defined as the volume fraction occupied by those micropores.[6] Thus, they have potential as low-*k* dielectric materials.

PSZs differ by their crystalline structure, microporosity and their framework density defined as the number of tetrahedrally coordinated atoms per 1000 Å^3. For example, the MFI (Socony Mobile-five) porous structure has 0.55 nm wide sinusoidal channels along the *a*-axis and 0.53 nm wide straight channels along the *b*-axis.[6] The MEL (Socony Mobile-eleven) structure has 0.54 nm wide straight channels along both the *a*- and *b*-axes.[6] The framework density of PSZ MEL and MFI is 17.4 and 18.4, respectively.[6] The dielectric constant can thus be tuned by controlling the PSZ structure and/or film final porosity. Note that amorphous sol-gel mesoporous silica thin films are also being considered as their dielectric constant can be tuned by varying the porosity. Unfortunately, porosity increases are often associated with decreases in thermal conductivity which may result in thermal management challenges.

Zeolites are also considered for a wide range of other applications such as chemical separation, sensing, catalysis, or cooling.[7–10] For example, zeolites can be used for the development of sorption-based heat exchangers for heat recovery and cooling applications.[11–15] For all these applications, knowledge of the thermal conductivity of these materials is critical for design and thermal management purposes.

Several studies have focused on the thermal conductivity of powdered zeolites.[16–18] However, few have focused on zeolite thin films.[19,20] Greenstein *et al.*[19] and Hudiono *et al.*[20] performed measurements of the specific heat and thermal conductivity of MFI zeolite films from 150 to 450 K for various silicon to aluminum ratios. The MFI films investigated were synthesized by secondary growth through a seeded hydrothermal process. The authors reported a cross-plane thermal conductivity at room temperature of (i) 1.0 W m^{-1} K^{-1} for 20 μm thick and *c*-oriented PSZ MFI films deposited on silicon substrates[19] and (ii) 1.35 W m^{-1} K^{-1} for 10 μm thick and (*h*0*l*)-oriented PSZ MFI films on alumina substrates.[20] Differences in experimental measurements may be explained by the difference in film orientation as *c*-oriented films have both sets of channels in the in-plane direction responsible for larger thermal resistance in the cross-plane direction. Finally, Greenstein *et al.*[19]

a)Electronic mail: yushan.yan@ucr.edu.
b)Electronic mail: pilon@seas.ucla.edu.

performed lattice dynamical modeling to simulate the specific heat and thermal conductivity of PSZ MFI. Hudiono *et al.*[20] extended both the experimental and numerical studies to (*h*0*l*)-oriented MFI thin films with different atomic compositions by varying the silicon to aluminum ratios from 25 to infinity. In both cases, fitting of the phonon relaxation time associated with different phonon scattering mechanisms resulted in good match between numerical results and experimental data over the range of temperature and composition considered. Aluminum incorporation and the presence of nanopores were found to be the main factors responsible for decreases in thermal conductivity.[19,20]

The present study focused on experimental measurements of the room temperature cross-plane thermal conductivity of (i) PSZ MEL films prepared by spin coating of MEL nanoparticle suspensions and (ii) of several PSZ MFI films for comparison purposes. These films featured different crystallinity, porosity, and architecture. The results were compared with those previously reported for sol-gel templated mesoporous silica thin films.[21] Numerical simulations were not performed in the present study. One can expect results for PSZ MFI films to be similar to those obtained by Hudiono *et al.*[20] because of the similar nature and orientation of the films. However, the very complex structure of the MEL thin films, made of MEL nanoparticles embedded into a disordered silica matrix, makes realistic simulations very difficult if not impossible.

II. METHOD AND EXPERIMENTS

A. Sample film preparation

Synthesis of PSZ MFI and MEL thin films investigated in this study were previously described in detail.[1,6] The MFI films were prepared by *in situ* crystallization and were *b*-oriented. The synthesis of the MEL nanoparticles suspension which was spun onto the silicon substrates was a two-stage process.[6] The first stage consisted of a two days heating and stirring of a tetraethyl-orthosilicate based solution. The second stage corresponded to the growth of the MEL nanoparticles from the same solution in a convection oven at 114 °C. As the duration of the second stage of the synthesis increased, bigger and more numerous zeolite nanoparticles were produced. Finally, MEL zeolite thin films were obtained by spin coating the solution. The MEL and MFI films were made hydrophobic by vapor-phase silylation with trimethylchlorosilane.[6] Four different sets of MEL films corresponding to four different second stage synthesis times (15, 18, 21, and 24 h) were studied. The resulting PSZ MEL thin films were characterized by (i) their porosity, (ii) their relative crystallinity, and (iii) the nanocrystal yield. The relative crystallinity was defined as the ratio of the film's micropore volume to the micropore volume of a fully crystalline PSZ MEL microcrystal.[6] The nanocrystal yield was defined as the MEL nanocrystals mass fraction present in the suspension before spin coating.[6]

B. Film characterization

Characteristics of the PSZ MFI and MEL thin films have been reported in detail by Wang *et al.*[1] and Li *et al.*,[6] respectively. MFI porosity, pore volume and surface area were previously reported by Flanigen *et al.*[22] and Tang *et al.*[23] On the other hand, the relative crystallinity of PSZ MEL thin films, their pore volume and specific BET surface area as a function of second stage synthesis time were reported by Li *et al.*[6] Here, the values of these parameters for the films investigated were interpolated from those reported in previous studies. In the present work, MEL film thickness and porosity were measured by ellipsometry (UVISEL from Horiba Jobin Yvon). Porosity results from ellipsometry matched well with previous N_2 adsorption measurements performed on similar powder samples. Finally, PSZ MEL nanoparticle size was estimated using phase analysis light scattering (PALS) (ZetaPALS from Brookhaven Instruments Corp.).

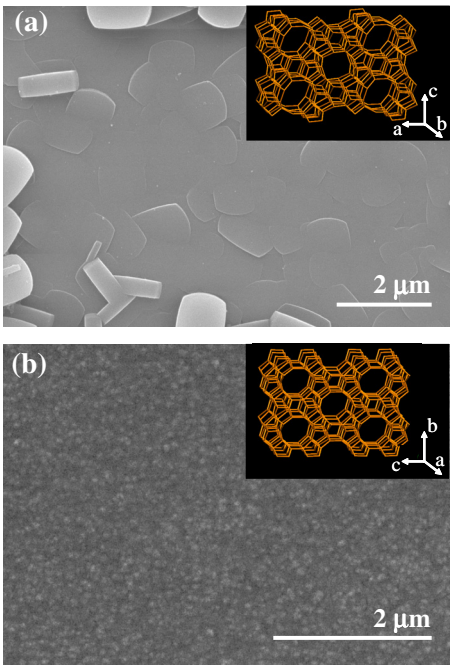

FIG. 1. (Color online) SEM images of (a) *in situ* PSZ MFI and (b) spin-on MEL (24 h) thin films. Loose crystals at the MFI thin film surface were polished away for thermal conductivity measurements. Insets show (a) the MFI framework viewed down the *b*-axis and (b) the MEL framework viewed down the *a*-axis (Ref. 31).

Figure 1(a) shows a SEM image of one of the PSZ MFI films investigated consisting of well-intergrown PSZ MFI crystals. Note that all PSZ MFI films were manually polished using an EcoMet polisher from Buehler to remove loose crystals at the surface of the films before thermal conductivity measurements. In addition, Fig. 1(b) shows a typical SEM image of the MEL films investigated consisting of PSZ MEL nanoparticles embedded in a nonuniform, disordered, and porous silica matrix.[24] The rms roughness of MEL films synthesized using the same process as that investigated was previously reported to be less than 5 nm.[6] The rms roughness of the PSZ MFI thin films, obtained after surface polishing, was not measured. However, comparison of SEM images suggests that it was lower than that of MEL thin films. Finally, unlike MFI films, MEL films featured also a mesoporosity corresponding to the volume fraction occupied by mesopores, 2.3 to 2.6 nm in diameter, located between the

TABLE I. Measured thermal conductivity and physical characteristics of the synthesized PSZ MEL and MFI thin films.

Sample No.	Structure	Second stage duration (h)	MEL particle size (± 1 nm)	Yield (± 1%)	Porosity (± 2%)	Total pore vol. ($cm^2\ g^{-1}$)	Micropore vol. ($cm^3\ g^{-1}$)	BET surface area ($m^2\ g^{-1}$)	Micropore area ($m^2\ g^{-1}$)	Thickness (nm)	Relative crystallinity (± 2%)	Thermal conductivity ($W\ m^{-1}\ K^{-1}$)
1	MFI	···	···	···	33[a]	0.19[b]	0.19[b]	457[b]	457[b]	320	100	0.93 ± 0.05
2	MFI	···	···	···	33[a]	0.19[b]	0.19[b]	457[b]	457[b]	350	100	1.03 ± 0.04
3	MFI	···	···	···	33[a]	0.19[b]	0.19[b]	457[b]	457[b]	310	100	1.12 ± 0.02
4	MFI	···	···	···	33[a]	0.19[b]	0.19[b]	457[b]	457[b]	310	100	0.99 ± 0.01
5	MEL	15	55	16	40	0.60[c]	0.033[c]	691[c]	86[c]	350	23[c]	1.05 ± 0.10
6	MEL	15	55	16	40	0.60[c]	0.033[c]	691[c]	86[c]	330	23[c]	0.80 ± 0.03
7	MEL	15	55	16	40	0.60[c]	0.033[c]	691[c]	86[c]	370	23[c]	1.09 ± 0.07
8	MEL	18	60	20	45	0.70[c]	0.048[c]	750[c]	119[c]	310	33[c]	1.02 ± 0.06
9	MEL	18	60	20	45	0.70[c]	0.048[c]	750[c]	119[c]	300	33[c]	0.87 ± 0.06
10	MEL	18	60	20	45	0.70[c]	0.048[c]	750[c]	119[c]	300	33[c]	1.17 ± 0.03
11	MEL	21	70	38	58	0.80[c]	0.060[c]	852[c]	143[c]	280	44[c]	1.01 ± 0.07
12	MEL	21	70	38	58	0.80[c]	0.060[c]	852[c]	143[c]	280	44[c]	1.07 ± 0.05
13	MEL	21	70	38	58	0.80[c]	0.060[c]	852[c]	143[c]	270	44[c]	1.01 ± 0.07
14	MEL	21	70	38	58	0.80[c]	0.060[c]	852[c]	143[c]	270	44[c]	1.06 ± 0.00
15	MEL	24	80	55	59	0.83[c]	0.068[c]	889[c]	149[c]	330	47[c]	0.99 ± 0.02
16	MEL	24	80	55	59	0.83[c]	0.068[c]	889[c]	149[c]	390	47[c]	0.95 ± 0.02
17	MEL	24	80	55	59	0.83[c]	0.068[c]	889[c]	149[c]	310	47[c]	0.91 ± 0.02

[a]From Flanigen *et al.* Ref. 22.
[b]From Tang *et al.* Ref. 23.
[c]Interpolated from Li *et al.* Ref. 6.

disordered silica matrix and the MEL nanoparticles.[25] The mesoporosity accounted for 91% to 94% of the MEL films total porosity.[6]

C. Thermal conductivity measurements

The cross-plane thermal conductivity of the PSZ MEL and MFI thin films was measured at room temperature using the 3ω method.[26] Principles, experimental apparatus and procedure as well as their validation have already been described elsewhere.[21] In brief, a conductive metallic wire, serving as both a thermometer and a line heat source, was patterned on top of the PSZ films. An ac current driven through the metallic wire generated temperature oscillations within the sample by Joule heating. Fluctuations in electrical resistance of the wire due to temperature variations were used to measure the amplitude of the film temperature oscillations. The thermal conductivity of the thin film was thus retrieved by analyzing the third harmonic voltage drop across the metallic wire.[26]

In this study, a metallic wire consisting of a 100 nm thick aluminum (Al) layer on top of a 10 nm thick chromium (Cr) layer [Cr(10 nm)/Al(100 nm)] was patterned on each sample surface and fabricated by photolithography, e-beam evaporation, and finally liftoff. The length and width of the metal wire were 1 mm and 30 μm, respectively. Note that the photolithographic process to pattern the metallic wire involves some strongly basic chemicals which can damage the zeolite thin films. Thus, a silicon nitride layer, less than 500 nm thick, was deposited on the zeolite films as a protective cap layer using plasma enhanced chemical vapor deposition (PECVD) before patterning the metallic heater. All samples were dried for more than 12 h at 150 °C before both nitride film PECVD deposition and thermal conductivity measurements to ensure no water was present in the pores. The thermal conductivity of at least three PSZ MEL thin film samples synthesized with the same second stage synthesis time was measured. Based on a previous study,[21] the uncertainty on the thermal conductivity measurements associated with the 3ω method was estimated to be ±15%. The latter accounts for potential errors due to both the sample film preparation and the various steps involved in the 3ω method, i.e., sample dehydration, variation in PECVD nitride film thickness and inhomogeneity, pattern resolution during photolithography, metal deposition, thickness and width during evaporation and lift-off, and finally bias errors in the 3ω electrical measurements.

III. RESULTS AND DISCUSSION

Table I summarizes the characteristics and the thermal conductivity measurements of all investigated PSZ MEL and MFI thin films. Four different second stage synthesis times for PSZ MEL samples were considered, namely 15, 18, 21, and 24 h. The film porosity ranged from 40% to 59%.[6,34] An absolute error of ±2% on porosity was obtained from repeated nitrogen adsorption/desorption experiments on similar powder samples. The nanocrystal yield was found to vary from 16 to 55% ± 1% and the nanocrystalline particle diameter from 55 to 80 nm ± 1 nm. Errors on those parameters correspond to the PALS measurement standard deviation and the variations observed on repeated weight measurements of the same samples, respectively. Finally, the corresponding relative crystallinity ranged from 23% to 47% with ±2% uncertainty. Note that the uncertainty for each of these parameters is absolute and that the relative difference between the 15, 18, 21, and 24 h samples should be independent of this uncertainty. The PSZ MEL films showed increasing (i) crystalline nanoparticle size and yield, (ii) porosity, and (iii) relative crystallinity as the second stage synthesis time in-

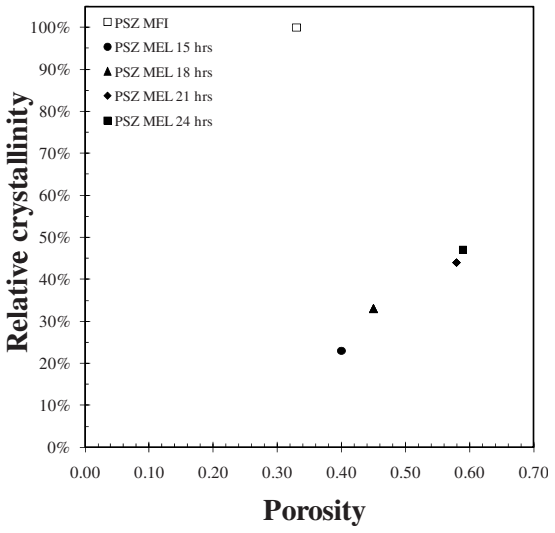

FIG. 2. Relative crystallinity as a function of porosity for PSZ MEL and MFI thin films (Ref. 21)

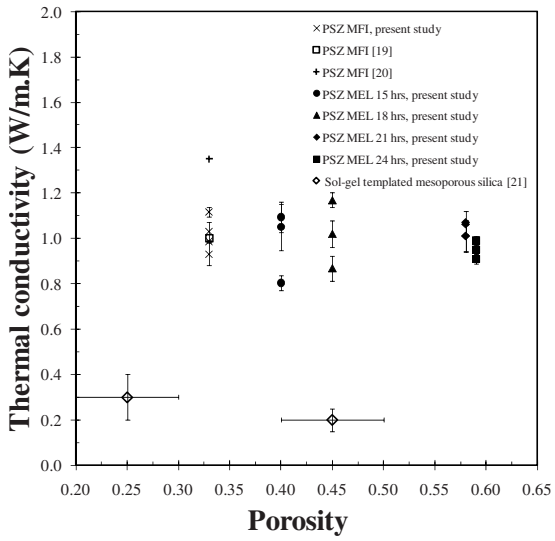

FIG. 3. Room temperature thermal conductivity of PSZ MEL and MFI thin films as a function of porosity, along with the average thermal conductivity previously reported for MFI films (Refs. 19 and 20) and for templated mesoporous silica thin films (Ref. 21).

creased. Figure 2 shows the linear relationship between relative crystallinity and porosity of the PSZ MEL thin films investigated.[31]

A. Effect of film thickness

All PSZ films synthesized in this study had thickness ranging from 270 to 390 nm (see Table I). The apparent thermal conductivity of thin films may depend on film thickness through the effect of the contact thermal resistance between the film and the substrate.[27] This dependence was not investigated in the present study. However, predictions could be made using (i) the model developed by Lee and Cahill [see Eq. (3) in Ref. 27] along with (ii) thermal contact resistance values previously reported for similar thin films.[21,27,28] For films thicker than 200 nm, thermal conductivity increased with film thickness at a rate less than 1.2%/100 nm. Therefore, for the range of thickness explored, its effect on the measured thermal conductivity can be assumed to be identical for all films. In other words, differences in thermal conductivity may be attributed only to changes in the nature of the PSZ films.

B. Effect of second stage synthesis time

Figure 3 shows the thermal conductivity of the PSZ MEL and MFI thin films as a function of porosity. Standard deviations observed for each samples as well as results of similar measurements reported in the literature for (i) PSZ MFI thin films[19,20] and for (ii) sol-gel templated mesoporous thin films[21] are also displayed. It indicates that despite important variations in porosity, the four different sets of PSZ MEL samples corresponding to different second stage synthesis times, exhibited similar thermal conductivity with an average value of 1.02 ± 0.03 W m^{-1} K^{-1}. Thermal conductivity of porous thin films is known to decrease dramatically with increasing porosity[21,29] and to increase with crystallinity.[30] Here, increases in relative crystallinity, crystalline nanoparticles' size, and yield, compensated for the effect of the simultaneous increase in porosity (Fig. 2) so that the thermal conductivity of the films remained nearly unchanged with second stage synthesis time. In addition, larger standard deviation was observed in the measurements for MEL samples obtained for second stage synthesis times of 15 and 18 h. This can be attributed to the fact that these samples corresponded to early stages of crystallization of the MEL nanoparticle suspension.[6]

C. Comparison between PSZ MEL and PSZ MFI films

The average thermal conductivity of the four PSZ MFI thin films investigated measured at room temperature was also found to be 1.02 ± 0.08 W m^{-1} K^{-1}. This is consistent with the value of 1.35 W m^{-1} K^{-1} reported by Hudiono *et al.*[20] for 10 μm thick and (*h0l*)-oriented PSZ MFI films. The larger thermal conductivity can be attributed to (i) differences in film synthesis and to (ii) the larger film thickness.

Moreover, thermal conductivity of the PSZ MEL thin films was similar to that of the PSZ MFI thin films. Yet, compared with MEL films, MFI films were oriented, 100% crystalline and had lower porosity and larger crystal size. Thus, one would expect PSZ MFI films to have a larger thermal conductivity than PSZ MEL films. This apparent contradiction might first be explained by uncertainties in porosity measurements. However, porosity of MFI thin films can be assessed from (i) optical measurements or (ii) the combination of effective density and adsorption measurements.[22] For instance, Flanigen *et al.*[22] and Tang *et al.*[23] reported a total specific pore volume of 0.19 cm^3 g^{-1} along with an effective density of 1.76 g^{-1} cm^3 for MFI. This agrees with MFI's theoretical density value calculated from framework density[31] and yields a porosity of 33% as porosity (=density × specific total pore volume). This porosity is also in agreement with results from the Maxwell Garnett model[32] applied to MFI with refractive index reported to be 1.39 (Ref. 22) and a solid matrix with refractive index of quartz equal to 1.543 at 627.8 nm.[33] Finally, MEL thin film

porosity measurements were also in good agreement with previous nitrogen adsorption measurements on powder samples.[6,34]

The fact that thermal conductivity of *in situ* MFI thin films was the same as that of spin on MEL thin films can be attributed to their much larger microporosity. Despite having a lower total porosity, MFI thin films have microporosity three to six times larger than MEL thin films (see Table I) resulting in a large pore surface area and small interpore distances. PSZ thermal conductivity is thus limited by phonon scattering on micropores. This becomes more important as (i) the pore surface area increases and as (ii) the phonon mean free path becomes comparable to the interpore distance.[35–38] This was already established by Hudiono *et al.*[20] who showed that the thermal conductivity of MFI was dominated by boundary like scattering at the pore interfaces.

D. Comparison with sol-gel templated mesoporous SiO_2 films

Figure 3 also shows that the average thermal conductivity of the PSZ MEL and MFI thin films was three to five times larger than that of sol-gel templated mesoporous silica thin films of similar porosity.[21] This can be attributed to the crystalline nature of the PSZ films. Note that the effect of pore size on thermal conductivity observed on PSZ thin films was not observed on sol-gel mesoporous silica thin films[21] because the latter (i) had an amorphous matrix as well as (ii) larger pores and interpore distance.

Thermal conductivity of MFI was found to be dominated by phonon scattering by the pores.[20] Moreover, the effective distance traveled by phonons between two consecutive scattering events was estimated to be around 4.8 nm (Ref. 20) which is approximately the length scale of the MFI pore network. On the other hand, interpore distances in sol-gel amorphous silica materials was ~3–12 nm (Ref. 21) and remained much larger than the coherent length [~0.6 nm (Ref. 39)] of the nonpropagating vibrational modes responsible for the heat conduction in the material.[21,40] Thermal conductivity of amorphous silica is thus less sensitive to pore size than that of MFI crystals.

E. Comparison of thermal and dielectric properties

The dielectric constants of PSZ MFI and MEL thin films investigated in this study were previously reported by Wang *et al.*[1] and Li *et al.*,[6] respectively. The dielectric constant of spin-on MEL thin films decreased from 2.4 to 1.9 as the second stage synthesis time increased from 15 to 24 h.[6] It was lower than that of *in situ* MFI thin films which was reported to equal 2.7.[1] The present study establishes that the dielectric constant of MEL thin films can be reduced without significantly decreasing the film's thermal conductivity. Furthermore, dielectric constant as low as 1.5 was reported for PSZ MEL thin films with porosity of 64%.[34] This dielectric constant is as low as that of sol-gel templated mesoporous silica thin films of similar porosity.[41–43] However, the latter have much lower thermal conductivity.[21] Note that PSZ and sol-gel templated mesoporous silica materials are often considered for similar applications. PSZ films appear to be better candidates for applications where thermal management is critical such as in low-*k* dielectrics for VLSI circuits. Mesoporous silica films should be preferred for thermal insulation, for example.

IV. CONCLUSION

This paper presented experimental measurements of the cross-plane thermal conductivity of PSZ MEL and MFI thin films at room temperature. PSZ MEL thin films were obtained by spin coating of MEL nanoparticle suspensions. PSZ MFI thin films were synthesized by *in situ* crystallization and were *b*-oriented. For MEL thin films, no significant changes in thermal conductivity were observed as the crystallization time used to grow the MEL nanoparticles increased. Indeed, the effect of increasing porosity on the thermal conductivity was compensated by the effects of the simultaneous increases in relative crystallinity, crystalline nanoparticle size, and yield. In spite of being less porous and fully crystalline, MFI thin films had the same thermal conductivity as spin-on MEL thin films. This was attributed to the large surface area of the micropores and small interpore distance in the MFI films. Finally, PSZ MEL thin films feature dielectric constants as low as that of sol-gel templated mesoporous silica thin films of identical porosity but their thermal conductivity was found to be five times larger.

[1] Z. Wang, H. Wang, A. Mitra, L. Huang, and Y. Yan, Adv. Mater. (Weinheim, Ger.) **13**, 746 (2001).
[2] K. Maex, M. R. Baklanov, D. Shamiryan, F. Iacopi, S. H. Brongersma, and Z. S. Yanovit-skaya, J. Appl. Phys. **93**, 8793 (2003).
[3] Semiconductor Industry Association, "The international technology roadmap for semiconductors," 2009.
[4] W. Volksen, R. D. Miller, and G. Dubois, Chem. Rev. **110**, 56 (2010).
[5] P. S. Ho, W. W. Lee, and J. J. Leu, *Low Dielectric Constant Materials for IC Applications* (Springer, New York, 2003), Vol. 9.
[6] Z. Li, C. M. Lew, S. Li, D. I. Medina, and Y. Yan, J. Phys. Chem. B **109**, 8652 (2005).
[7] J. P. Dong, J. Zou, and Y. C. Long, Microporous Mesoporous Mater. **57**, 9 (2003).
[8] M. E. Davis, Nature (London) **417**, 813 (2002).
[9] Z. Lai, G. Bonilla, I. Diaz, J. G. Nery, K. Sujaoti, M. A. Amat, E. Kokkoli, O. Terasaki, R. W. Thompson, M. Tsapatsis, and D. G. Vlachos, Science **300**, 456 (2003).
[10] C. M. Lew, R. Cai, and Y. Yan, Acc. Chem. Res. **43**, 210 (2010).
[11] M. Tatlier and A. E. Erdem-Sematalar, Chem. Eng. Commun. **180**, 169 (2000).
[12] J. M. Gordon, K. C. Ng, H. T. Chua, and A. Chakraborty, Int. J. Refrig. **25**, 1025 (2002).
[13] A. O. Dieng and R. Z. Wang, Renewable Sustainable Energy Rev. **5**, 313 (2001).
[14] R. A. Munoz, D. Beving, and Y. Yan, Ind. Eng. Chem. Res. **44**, 4310 (2005).
[15] J. Liu, G. Aguilar, R. Munoz, and Y. Yan, AIChE J. **54**, 779 (2008).
[16] V. V. Murashov and M. A. White, Mater. Chem. Phys. **75**, 178 (2002).
[17] Z. Y. Liu, G. Cacciola, G. Restuccia, and N. Giordano, Zeolites **10**, 565 (1990).
[18] M. B. Jakubinek, Microporous Mesoporous Mater. **103**, 108 (2007).
[19] A. M. Greenstein, S. Graham, Y. C. Hudiono, and S. Nair, Nanoscale Microscale Thermophys. Eng. **10**, 321 (2006).
[20] Y. Hudiono, A. Greenstein, C. Saha-Kuete, B. Olson, S. Graham, and S. Nair, J. Appl. Phys. **102**, 053523 (2007).
[21] T. Coquil, E. K. Richman, N. Hutchinson, S. H. Tolbert, and L. Pilon, J. Appl. Phys. **106**, 034910 (2009).
[22] E. M. Flanigen, Nature (London) **271**, 512 (1978).
[23] Z. Tang, J. Dong, and T. M. Nenoff, Langmuir **25**, 4848 (2009).
[24] Y. Liu, C. M. Lew, M. Sun, R. Cai, J. Wang, G. Kloster, B. Boyanov, and Y. Yan, Angew. Chem., Int. Ed. **48**, 4777 (2009).

[25]S. Li, J. Sun, Z. Li, H. Peng, D. Gidley, E. T. Ryan, and Y. Yan, J. Phys. Chem. B **108**, 11689 (2004).
[26]D. G. Cahill, Rev. Sci. Instrum. **61**, 802 (1990).
[27]S. M. Lee and D. G. Cahill, J. Appl. Phys. **81**, 2590 (1997).
[28]T. Yamane, N. Nagai, S. I. Katayama, and M. Todoki, J. Appl. Phys. **91**, 9772 (2002).
[29]C. Hu, M. Morgen, P. S. Ho, A. Jain, W. N. Gill, J. L. Plawsky, and P. C. Wayner, Appl. Phys. Lett. **77**, 145 (2000).
[30]Z. Huang, Z. Tang, J. Yu, and S. Bai, Physica B **404**, 1790 (2009).
[31]C. Baerlocher and L. B. McCusker, "Database of zeolite structures," http://www.iza-structure.org/databases/
[32]N. Hutchinson, A. Navid, T. Coquil, and L. Pilon, Thin Solid Films **518**, 2141 (2010).
[33]Optical Society of America, *Handbook of Optics* (McGraw-Hill, New York, 1994), Vol. 2.
[34]Z. Li, M. C. Johnson, M. Sun, E. T. Ryan, D. J. Earl, W. Maichen, J. I. Martin, S. Li, C. M. Lew, J. Wang, M. W. Deem, M. E. Davis, and Y. Yan, Angew. Chem., Int. Ed. **45**, 6329 (2006).
[35]A. Majumdar, ASME J. Heat Transfer **115**, 7 (1993).
[36]I. Sumirat, Y. Ando, and S. Shimamura, J. Porous Mater. **13**, 439 (2006).
[37]R. Prasher, J. Appl. Phys. **100**, 064302 (2006).
[38]J. D. Chung and M. Kaviany, Int. J. Heat Mass Transfer **43**, 521 (2000).
[39]C. Kittel, *Introduction to Solid State Physics*, 7th ed. (Wiley, New York, 1996).
[40]J. L. Feldman, M. D. Kluge, P. B. Allen, and F. Wooten, Phys. Rev. B **48**, 12589 (1993).
[41]F. K. de Theije, A. R. Balkenende, M. A. Verheijen, M. R. Baklanov, K. P. Mogilnikov, and Y. Furukawa, J. Phys. Chem. B **107**, 4280 (2003).
[42]S.-B. Jung, C.-K. Han, and H.-H. Park, Appl. Surf. Sci. **244**, 47 (2005).
[43]R. A. Farrell, K. Cherkaoui, N. Petkov, H. Amenitsch, J. D. Holmes, P. K. Hurley, and M. A. Morris, Microelectron. Reliab. **47**, 759 (2007).